Journal of Cerebral Blood Flow & Metabolism (2011) 31, 2030–2040
© 2011 ISCBFM All rights reserved 0271-678X/11
www.jcbfm.com

JCBFM Open

Cilostazol minimizes venous ischemic injury in diabetic and normal rats

Daisuke Wajima, Mitsutoshi Nakamura, Kaoru Horiuchi, Yasuhiro Takeshima, Fumihiko Nishimura and Hiroyuki Nakase

Department of Neurosurgery, Nara Medical University School of Medicine, Nara, Japan

We evaluated the effects of cilostazol on venous infarction produced by a photothrombotic two-vein occlusion (2VO) model in diabetic and control rats. The cerebral blood flow (CBF) between the occluded veins was measured by laser Doppler flowmetry for 4 hours after 2VO. Infarct size and immunohistochemistry were evaluated 24, 48, 96, and 168 hours after 2VO. Cilostazol was administered 1 hour after 2VO, and thereafter at a continuous oral dose of 60 mg/kg per day. Cilostazol reduced the infarct size, and the number of terminal deoxynucleotidyl transferase-mediated deoxyuridine triphosphate nick-end labeling (TUNEL)-positive apoptotic and B-cell lymphoma 2-associated X protein (Bax)-positive cells, and improved the CBF in control rats. In diabetic rats, cilostazol reduced the infarct size, and the number of TUNEL-positive apoptotic and Bax-positive cells, 96 and 168 hours after 2VO, but did not improve the CBF 4 hours after 2VO. Cilostazol increased the number of B-cell lymphoma 2 (Bcl-2)-positive cells in both strains 48, 96, and 168 hours after 2VO, but did not improve vessel wall thickness or collagen deposits. Cilostazol appeared to limit venous infarcts by improving the penumbral CBF in nondiabetic rats, and inhibited pro-apoptotic changes through Bcl-2 overexpression, without improving the CBF in diabetic rats.
Journal of Cerebral Blood Flow & Metabolism (2011) **31,** 2030–2040; doi:10.1038/jcbfm.2011.47; published online 20 April 2011

Keywords: cilostazol; diabetes; OLETF rats; two-vein occlusion; venous infarction

Introduction

Cilostazol is a selective inhibitor of phosphodiesterase-3, which acts as an antiplatelet drug and a vasodilator. It has been used for the treatment of ischemic symptoms in patients with chronic peripheral arterial obstruction, and for the secondary prevention of brain infarction. Recently, cilostazol was shown to be a more effective and safer alternative to aspirin for the long-term prevention of secondary stroke in chronic ischemic stroke patients (Shinohara *et al*, 2010). Furthermore, cilostazol attenuated acute brain infarction induced by middle cerebral artery occlusion-reperfusion (MCAO-R) in rats, suggesting that it might have the potential to ameliorate acute ischemic stroke by minimizing evolving ischemic injury (Ito *et al*, 2009). However, the effect of cilostazol on venous infarction remains unknown, especially in the diabetic state.

Epidemiological studies have showed that diabetes is a risk factor for the development of ischemic cerebrovascular disease (Whisnant, 1997). Diabetes is associated with a series of vascular alterations, including intracranial atheroma, microangiopathy, cerebrovascular atherosclerosis, rheological abnormalities, and endothelial changes, any or all of which are predisposing factors for cerebral infarction (Vinik and Flemmer, 2002). The morbidity and mortality associated with diabetes have traditionally been attributed to the chronic complications affecting both the large vessels, with an increased risk of myocardial infarction and stroke, and the microvasculature of the kidneys, retinas, and peripheral nerves. Recently, we showed that the volume of the cerebral cortex affected by venous infarction was increased in diabetic rats, and we also observed significantly reduced cerebral blood flow (CBF) 90 minutes after venous infarction, coupled with increased apoptosis in and around ischemic lesions. Morphologically, diabetic rats showed marked thickening of the walls of the small cerebral vessels along with perivascular fibrosis, indicating more severe cerebral microvascular atherosclerotic changes than those observed in their nondiabetic counterparts (Wajima *et al*, 2010).

Correspondence: Dr H Nakase, Department of Neurosurgery, Nara Medical University School of Medicine, 840 Shijo-cho, Kashihara, Nara 634-8521, Japan.
E-mail: nakasehi@naramed-u.ac.jp
This work was supported by a Grant-in-Aid for Scientific Research from the Ministry of Education, Culture, Sports, Science, and Technology of Japan (no. 22791352).
Received 25 November 2010; revised 16 February 2011; accepted 17 March 2011; published online 20 April 2011

Two-vein occlusion (2VO) provides a unique and reliable model of cerebral venous-circulation disturbance involving the photochemically induced occlusion of two adjacent cortical veins in the rat brain, in which endothelial alteration stimulates platelet activation resulting in a venous thrombus (Nakase *et al*, 1996). The 2VO model causes a relatively widespread reduction of cortical flow and the development of small infarcts. It mimics conditions similar to those expected to occur in an ischemic penumbra zone, and has distinct advantages over other arterial occlusion models (Nishioka *et al*, 2006). Here, we used the 2VO model to examine the effect of cilostazol in minimizing evolving ischemic injury in both nondiabetic and diabetic rats.

Materials and methods

Animal Preparation

Male 4-week-old spontaneously diabetic Otsuka Long-Evans Tokushima Fatty (OLETF) rats and control Long-Evans Tokushima Otsuka (LETO) rats were supplied by the Tokushima Research Institute (Otsuka Pharmaceutical, Tokushima, Japan). In total, 40 OLETF and 40 LETO rats were maintained in a temperature-controlled room at $23 \pm 2^{\circ}C$ with $55 \pm 15\%$ humidity and a 12-hours light/dark cycle. The animals were provided standard rat chow and tap water *ad libitum*, and were housed under husbandry standards that were in accordance with the ethical guidelines of our institution. The experimental protocol was approved by the Animal Welfare Committee of Nara Medical University, Japan, and was conducted in compliance with the Animal Experiment Guidelines approved by the 89th General Assembly of the Japan Science Council in 1980.

An oral glucose-tolerance test was performed on each rat at 30 weeks of age to determine the diabetic status. After 16-hours fast, an oral glucose load of 2 g/kg was delivered to each rat via gavage. Blood glucose levels were measured before gavage, and at 30, 60, 90, and 120 minutes after glucose loading, using a standard skin-prick blood glucometer (Medi-safe Mini; TERUMO, Tokyo, Japan). Animals were classified as diabetic if the peak plasma glucose level was >300 mg/dL and if the measurement remained at >200 mg/dL for 120 minutes (Kawano *et al*, 1992).

Anesthesia

After the diabetic status had been determined, each rat was sedated with 1 mg atropine and initially anesthetized by an intraperitoneal injection of chloral hydrate at 36 mg/100 g body weight. Tracheal intubation was performed after relaxation, and ventilation was controlled by a small animal respirator (Harvard Model 683; Harvard Apparatus, MA, USA). The rats were then anesthetized with halothane (2% for induction and 1% for maintenance) in a mixture of 70% nitrous oxide and 30% oxygen. The rectal temperature was maintained at $37^{\circ}C$ with a feedback heating pad (CMA 150; Carnegie Medicine AB, Stockholm, Sweden). Polyethylene catheters were inserted into the tail artery and the left femoral vein. Blood gas parameters, including the partial pressure of oxygen (PaO_2) and the partial pressure of carbon dioxide ($PaCO_2$), as well as the arterial pH, blood pressure, and glucose concentration, were continuously monitored through the intraarterial catheter connected to a pressure transducer (ABL 550; Radiometer, Copenhagen, Denmark), while the venous line was used to administer fluids and drugs.

Craniotomy

The anesthetized rats were secured in stereotactic frames (SR-6; Narishige Inc., Tokyo, Japan) for the duration of the experiment. After performing a 1.5-cm midline skin incision, we prepared a left fronto-parietal cranial window using a high-speed drill for access to the brain surface. The entire procedure was performed with the aid of an operating microscope (Carl Zeiss, Oberkochen, Germany). During the craniotomy, the drill tip was cooled continuously with physiological saline to avoid thermal injury to the cortex. The dura mater was left intact. As a control, we performed three sham operations without inducing photochemical thrombosis, and were able to confirm that the intact brain showed no notable changes compared with the nonoccluded side in the animals with induced thrombosis.

Cortical Vein Occlusion by Photochemically Induced Thrombosis and Medication

We performed 2VO according to the method described in previous reports (Kimura *et al* 2005; Nakagawa *et al*, 2005; Nakase *et al*, 1996; Nishioka *et al*, 2006; Otsuka *et al*, 2000; Wajima *et al*, 2010). Briefly, we occluded two adjacent cortical veins using a rose bengal dye injection (Katayama Chemicals, Osaka City, Japan), followed by illumination by the L4887 fiber-optic system (6,500 to 7,500 lux, 540 nm; Hamamatsu Photonics, Hamamatsu, Japan) with a 100-μm fiber. The rose bengal dye (50 mg/kg) was injected slowly into the first selected cortical vein to avoid affecting the systemic arterial pressure, followed by exposure to light for 10 minutes with the aid of a micromanipulator-assisted light guide. Care was taken to avoid any illumination of the tissue and vessels near the target vein. To occlude the second selected vein, rose bengal dye (25 mg/kg) was injected intravenously followed by illumination as described above (Nakase *et al*, 1996). The regional CBF was measured, using a laser Doppler flowmeter (ALF21; Advance, Inc., Tokyo, Japan) with a 0.8-mm needle probe, at 25 locations within the occluded veins lateral to the scanning field, and the mean value was calculated. The CBF was measured before the 2VO and then at 30-minutes intervals until 4 hours after the intervention. We administered the drug 60 minutes after 2VO. Rats were orally administered either cilostazol (60 mg/kg per day) or 0.5% carboxymethyl cellulose (CMC) sodium salt vehicle alone as a control. After the closure of the incisions, the rats were returned to their individual cages with free access to food and water, and they continued to receive medication once

daily for 7 days. The drug dosage was based on a previous study of the MCAO model in rats (Lee *et al*, 2008).

Histopathology

At 24, 48, 96, and 168 hours after 2VO, rats were killed after being anesthetized by an intraperitoneal injection of chloral hydrate, followed by perfusion fixation initiated by the transcardiac infusion of saline followed by 10% formaldehyde. The brains were excised and coronal blocks from the middle frontal cortex tissue, containing the two occluded cortical cerebral veins, were paraffin processed. Sections with a thickness of 5 μm were cut and stained with hematoxylin and eosin for examining the overall morphology. Additional sections were cut for Van Gieson's elastic and immunohistochemical staining, and serial sections were prepared for terminal deoxynucleotidyl transferase-mediated deoxyuridine triphosphate nick-end labeling (TUNEL).

Calculation of the Infarct Ratio

The infarct area was measured in brain slices by quantitative histomorphometry in a blinded manner. The infarct and hemispheric areas of each section were traced and measured by an image-analysis system using a Windows computer accessing the public domain National Institutes of Health Image program, Scion Image. The percentage of infarct area (the infarct ratio) was calculated by dividing the infarct area by the total area of the ipsilateral hemisphere. The infarct area was evaluated in serial sections at 200-μm steps. The infarct volume was calculated as the sum of these areas and was expressed as the infarct ratio.

Van Gieson's Elastic Staining

Brain sections were subjected to Van Gieson's elastic staining to examine the peri-vascular collagen deposition. Vessel cross-sections with a long axis to short axis ratio of $<1:3$ were used for evaluation and quantitative scoring, based on our previous study of the vessels of diabetic rats (Wajima *et al*, 2010). Peri-vascular fibrosis was assessed by the ratio of vascular collagen to the total vessel area (the area of collagen deposition/the total vessel area), in which the total vessel area was defined as the sum of the tunica media and the vessel lumen.

Immunohistochemistry

For the immunohistochemical analysis, unstained sections of the cerebral cortex were deparaffinized and heated in citrate buffer for 5 minutes at 120°C in an autoclave. Endogenous peroxidase activity was blocked by incubation in 0.3% hydrogen peroxide (H_2O_2), and the sections were incubated overnight with mouse monoclonal antibodies directed against smooth muscle actin (SMA; Santa Cruz Biochemicals, Santa Cruz, CA, USA; 1:100 dilution), B-cell lymphoma 2-associated X protein (Bax; SC7480; Santa Cruz Biochemicals; 1:500 dilution), B-cell lymphoma 2 (Bcl-2; SC7480; Santa Cruz Biochemicals; 1:300 dilution), and advanced glycation end products (AGEs; 6D12; TransGenic Inc., Kumamoto, Japan; 1:20 dilution).

The vascular cross-sections in the SMA-stained slides were quantitatively analyzed, and the ratio of the tunica media to the lumen (wall area/luminal area) was calculated as an index of wall thickening. The percentages of Bax- and Bcl-2-immunopositive cells within the penumbral lesions in the ischemic cerebral tissues, and of AGE-immunopositive cells within the nonischemic cerebral tissues, were estimated from the average number of cells in three sections per rat within a 5-mm^2 area of the cortex.

Terminal Deoxynucleotidyl Transferase-Mediated Deoxyuridine Triphosphate Nick-End Labeling Staining

The DNA-fragmentation characteristics of cells undergoing apoptosis were assessed by the TUNEL method in accordance with the instructions for the ApopTag kit (Oncor, Inc., Gaithersburg, MD, USA) with minor modifications. Briefly, after deparaffinization and rehydration, serial sections were digested with 20 mg/mL proteinase K (Sigma, St Louis, MO, USA) for 15 minutes at room temperature, followed by exposure to terminal deoxynucleotidyl transferase (Nichirei, Tokyo, Japan) in a reaction buffer containing fixed concentrations of digoxigenin-labeled nucleotides at 37°C for 1 hour. The slides were then placed in a stop/wash buffer for 10 minutes, and subsequently incubated with antidigoxigenin-labeled peroxidase for 30 minutes and counterstained with hematoxylin. Diaminobenzidine-stained cells were identified as TUNEL positive.

The percentages of TUNEL-positive cells within these penumbral areas were estimated using the mean number of TUNEL-positive cells in three sections per rat within a 5-mm^2 area of the cortex, using the method described above for Bax/Bcl-2 immunohistochemistry.

Statistical Analysis

All data are expressed as the mean ± s.e.m. Statistical significance (at $P<0.05$) was assessed using the Student–Newman–Keuls test with repeated-measures analysis of variance for data on CBF and physiological parameters, with two-way analysis of variance for data on vessel wall histopathology, and with one-way analysis of variance for all other data. All statistical analyses were performed by Sigma-Stat software (Jandel Scientific, San Rafael, CA, USA).

Results

Body Weight and Oral Glucose-Tolerance Test

At 30 weeks of age, the 40 OLETF rats were significantly heavier than the 40 LETO rats (587 ± 12 versus 352 ± 15 g, respectively; $P<0.01$). The oral glucose-tolerance test revealed significantly

elevated fasting glucose levels in the OLETF rats compared with the LETO rats (114.6 ± 4.1 versus 75.4 ± 4.1 mg/dL, respectively; $P < 0.05$), as well as significant increases in the peak glucose response (326.5 ± 11.3 versus 141.2 ± 6.1 mg/dL, respectively; $P < 0.01$). Moreover, the glucose levels remained significantly higher in the OLETF rats than in the LETO rats at 120 minutes after administration (254.4 ± 3.2 versus 122.1 ± 4.6 mg/dL, respectively; $P < 0.05$). In light of previous findings (Kawano *et al*, 1992), this indicates that OLETF rats are diabetic by 30 weeks of age, whereas the glucose levels of LETO rats remain within the normal range.

Sequential Changes in Regional Cerebral Blood Flow

The sequential changes in the regional CBF of the OLETF rats during 2VO are shown in Figure 1. Before 2VO, the regional CBF between the two occluded veins was similar in the LETO and OLETF rats (31.7 ± 0.8 versus 31.6 ± 0.8 laser Doppler units, respectively). The CBF was subsequently calculated and expressed as a percentage of the initial value (% baseline). The CBF decreased over time in the cilostazol-administered and vehicle-administered OLETF rats (71.0 ± 2.7% versus 70.2 ± 1.8% at 30 minutes after 2VO and 12.2 ± 2.6 versus 9.5 ± 2.7% at 240 minutes, respectively). Similarly, the CBF decreased in both the cilostazol-administered and the vehicle-administered LETO rats until 90 minutes after 2VO (71.0 ± 1.8% versus 71.2 ± 2.1% at 30 minutes and 35.7 ± 2.4% versus 35.2 ± 1.9% at 90 minutes, respectively). However, compared with the control LETO rats, cilostazol inhibited the reduction of the CBF in the LETO rats at 120 minutes (31.3 ± 2.8% versus 35.4 ± 3.6%, $P < 0.05$) and 240 minutes (28.5 ± 2.3% versus 42.1 ± 2.8%, $P < 0.05$) after its administration, respectively.

Physiological Parameters

There were no significant differences between the two groups in the mean arterial blood pressure, pH, PaO_2, $PaCO_2$, and hematocrit (Ht) values either before or after 2VO; however, the blood glucose concentrations were significantly higher in the OLETF rats than in the LETO rats at 240 minutes after 2VO (Table 1). The physiological parameters (other than the glucose concentration) measured before 2VO, and every 30 minutes until 4 hours after 2VO, did not significantly differ between the strains (Table 1).

Histology, Immunohistochemistry, and Terminal Deoxynucleotidyl Transferase-Mediated Deoxyuridine Triphosphate Nick-End Labeling Staining

Based on the histopathological findings, lesions in which the cells were reduced in number or were

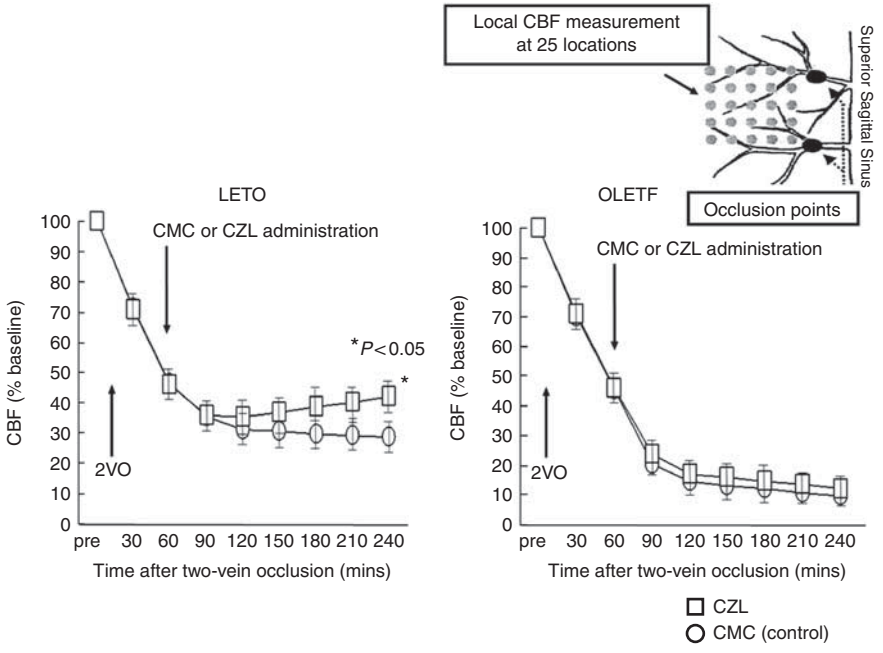

Figure 1 Comparison of rates of regional cerebral blood flow (CBF) in the ischemic areas of Otsuka Long-Evans Tokushima Fatty (OLETF) and Long-Evans Tokushima Otsuka (LETO) rats. Before two-vein occlusion (2VO), the regional CBF between the two occluded veins of the LETO and OLETF rats was similar (31.7 ± 0.8 versus 31.6 ± 0.8 laser Doppler units (LDU), respectively). The CBF decreased over time in the OLETF rats. The CBF also decreased in both the cilostazol (CZL)-administered and the carboxymethyl cellulose (CMC)-administered groups until 90 minutes after 2VO; however, CZL inhibited the reduction of CBF at 1 hour after administration in the LETO rats. The CBF, which was calculated as the average value of those in 25 points in the ischemic lesion, is expressed as a percentage of the baseline value (% baseline). The points of occlusion and the locations of the regional CBF measurements by the laser Doppler flowmeter are shown in the lower right of the figure.

Table 1 Physiological data

	MABP (mm Hg)	*Pa_{O_2} (mm Hg)*	*Pa_{CO_2} (mm Hg)*	*pH*	*Ht (%)*	*Glucose (mg/dL)*
LETO						
Pre 2VO	108.6 ± 6.8	125.1 ± 7.5	42.9 ± 2.7	7.38 ± 0.04	45.1 ± 0.6	78.4 ± 4.3
30 minutes after 2VO	110.4 ± 4.9	120.1 ± 3.5	41.7 ± 1.8	7.37 ± 0.09	45.3 ± 1.1	85.4 ± 2.4
60 minutes after 2VO	111.6 ± 6.4	122.3 ± 6.2	42.3 ± 2.1	7.39 ± 0.11	45.8 ± 0.7	79.2 ± 3.1
90 minutes after 2VO	110.4 ± 3.5	123.1 ± 5.4	41.1 ± 1.5	7.41 ± 0.14	45.2 ± 0.6	88.4 ± 2.4
2 hours after 2VO	109.2 ± 5.3	121.8 ± 6.2	42.6 ± 1.2	7.36 ± 0.12	45.8 ± 1.2	75.9 ± 2.9
4 hours after 2VO	107.2 ± 5.9	124.0 ± 8.5	42.9 ± 2.1	7.37 ± 0.27	45.3 ± 0.6	83.2 ± 5.3
OLETF						
Pre 2VO	112.6 ± 5.5	124.1 ± 3.5	43.8 ± 3.1	7.41 ± 0.07	44.8 ± 1.1	318.4 ± 6.3*
30 minutes after 2VO	111.2 ± 3.8	122.0 ± 4.2	43.9 ± 3.4	7.40 ± 0.14	44.7 ± 0.9	342.0 ± 3.3*
60 minutes after 2VO	112.2 ± 4.1	125.0 ± 2.3	43.1 ± 4.1	7.39 ± 0.21	44.3 ± 0.6	328.2 ± 5.3*
90 minutes after 2VO	111.3 ± 4.8	123.1 ± 2.5	43.3 ± 2.7	7.39 ± 0.15	44.8 ± 0.7	326.4 ± 5.3*
2 hours after 2VO	110.6 ± 3.7	125.1 ± 4.2	43.2 ± 1.9	7.41 ± 0.24	44.4 ± 0.6	331.4 ± 4.2*
4 hours after 2VO	114.5 ± 4.3	124.1 ± 4.5	44.0 ± 1.7	7.38 ± 0.54	44.8 ± 0.6	342.4 ± 6.3*

2VO, two-vein occlusion; MABP, mean arterial blood pressure; Pa_{O_2}, partial pressure of oxygen; Pa_{CO_2}, partial pressure of carbon dioxide; Ht, hematocrit; OLETF, Otsuka Long-Evans Tokushima Fatty; LETO, Long-Evans Tokushima Otsuka.
All data are expressed as the mean ± s.e.m. Glucose concentrations were significantly higher in OLETF rats both before and after experimental venous occlusion (*$P < 0.01$). No other measures differed significantly between the two strains.

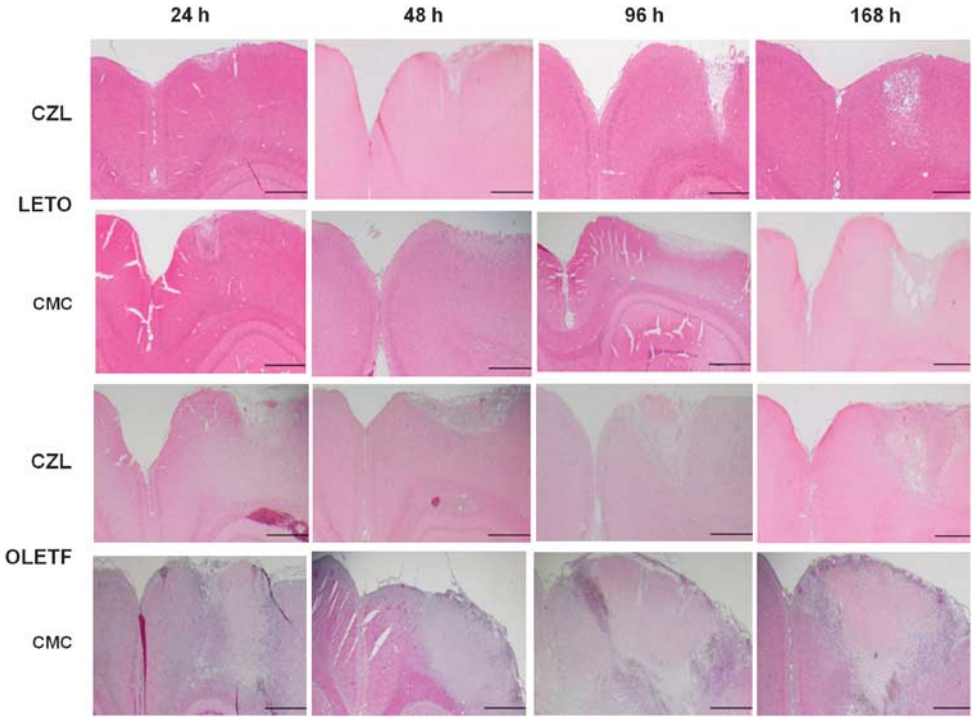

Figure 2 Hematoxylin and eosin (H&E) staining for cerebral damage induced by two-vein occlusion (2VO), and the effects of cilostazol (CZL) and carboxymethyl cellulose (CMC) in Long-Evans Tokushima Otsuka (LETO) and Otsuka Long-Evans Tokushima Fatty (OLETF) rats. The infarct cores, surrounded by penumbral zones, show morphological changes in the neurons (bar = 500 μm, × 40 magnification).

defective were identified as the infarct area, and lesions around the infarct core were identified as so-called penumbra. As shown in Figures 2 and 3, the venous infarct volume increased over time and was reduced by cilostazol in each of the five LETO rats tested (2.5 ± 0.4% versus 1.4 ± 0.3% at 24 hours after 2VO, 3.5 ± 0.3% versus 2.2 ± 0.6% at 48 hours, 5.1 ± 0.3% versus 3.5 ± 0.5% at 96 hours, and 5.5 ± 0.6% versus 3.7 ± 0.4% at 168 hours, respectively). Additionally, the infarct volume was increased in both treatment groups at 24 hours (8.2 ± 0.3% versus 7.1 ± 0.5%) and 48 hours (10.1 ± 0.6% versus 9.5 ± 0.3%) after 2VO in OLETF rats; however, cilostazol significantly reduced the

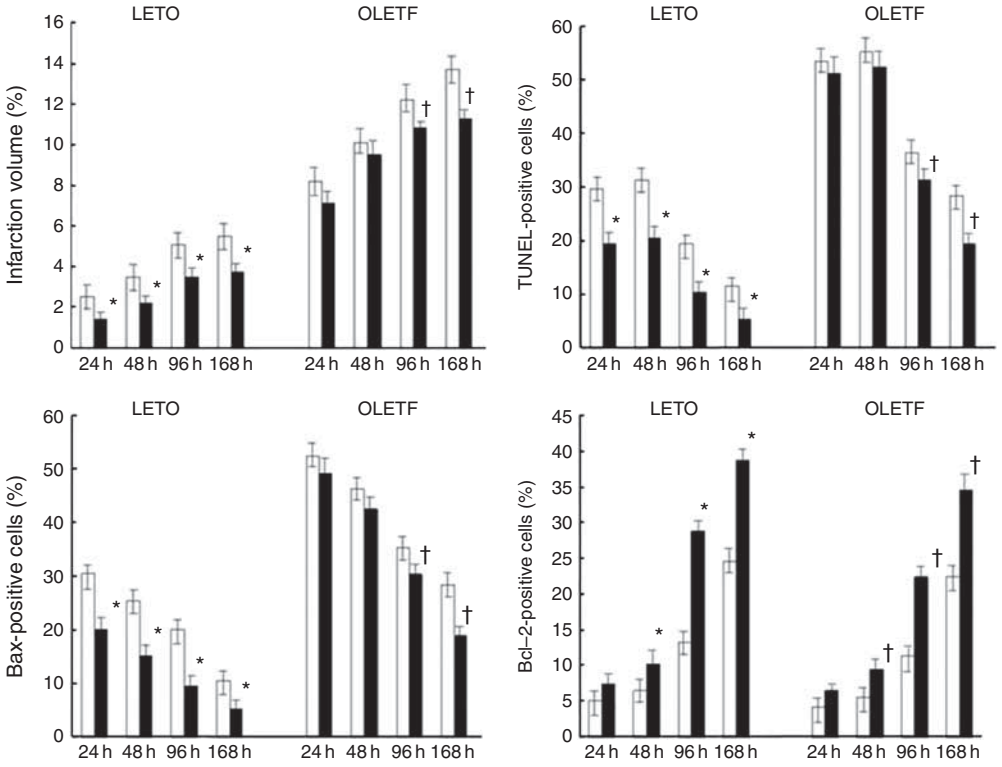

Figure 3 Infarct volume and rates of TUNEL-, Bax-, and Bcl-2-positive cells. The venous infarct volume was reduced by cilostazol in the Long-Evans Tokushima Otsuka (LETO) rats. In the Otsuka Long-Evans Tokushima Fatty (OLTEF) rats, the infarct volume increased up to 48 hours after two-vein occlusion (2VO), but was significantly reduced by cilostazol after 96 hours. The percentage of TUNEL-positive cells was higher, but was reduced significantly after 96 hours, in the OLETF rats, while it was significantly reduced by cilostazol in the LETO rats. The percentage of Bax-positive cells showed the same pattern. The percentage of Bcl-2-positive cells near the infarct area significantly increased 48 hours after cilostazol administration in both the LETO and the OLETF rats. The data for the cilostazol-administered groups are represented by dark bars and the data for the carboxymethyl cellulose (CMC)-administered groups are represented by light bars. TUNEL, terminal deoxynucleotidyl transferase-mediated deoxyuridine triphosphate nick-end labeling; Bax, B-cell lymphoma 2-associated X protein; Bcl-2, B-cell lymphoma 2.

infarct volume after 96 hours ($12.2 \pm 0.4\%$ versus $10.8 \pm 0.6\%$) and 168 hours ($13.7 \pm 0.6\%$ versus $11.3 \pm 0.5\%$), respectively. Hematoxylin and eosin staining revealed morphological changes in neurons in both the infarct cores and the surrounding penumbral areas. Furthermore, cells near to the penumbra showed histological morphological signs of apoptosis (such as nuclear pyknosis, chromatin condensation or fragmentation, and cytoplasmic shrinkage).

Vascular wall thickening and perivascular fibrosis, which are signs of atherosclerosis, were more notable in the OLETF rats than in the LETO rats. The relative thickness of the tunica media in the small cortical vessel walls of OLETF and LETO rats was highlighted by SMA staining. As illustrated in Figure 4, the ratio of the wall thickness to the luminal area was significantly higher in the OLETF rats than in the LETO rats. The wall thickness was not improved by cilostazol at 168 hours after 2VO in either the LETO rats ($43.3 \pm 1.2\%$ versus $42.4 \pm 1.4\%$) or the OLETF rats ($64.5 \pm 1.0\%$ versus $63.0 \pm 1.1\%$). Sections stained with Van Gieson's elastic further showed increased smooth muscle fibers and collagen in the OLETF rats, which had a significantly higher ratio of collagen-stained tissue to total vessel area compared with LETO rats (Figure 4); this change in the small vessels of both LETO rats ($28.6 \pm 1.8\%$ versus $27.8 \pm 1.5\%$) and OLETF rats ($48.5 \pm 1.7\%$ versus $45.9 \pm 1.9\%$) was not improved by cilostazol at 168 hours after 2VO.

Numerous TUNEL-positive cells, with darkly stained nuclei or nuclear fragments and cytoplasmic halos characteristic of apoptotic cells, were observed around the infarct area. As shown in Figure 5, the frequency of TUNEL-positive cells was greater in OLETF rats than in LETO rats, and was not reduced by cilostazol during the 48 hours after 2VO ($53.4 \pm 1.3\%$ versus $51.3 \pm 1.5\%$ at 24 hours and $55.2 \pm 1.1\%$ versus $52.4 \pm 0.8\%$ at 48 hours), but decreased significantly after 96 hours ($36.3 \pm 1.4\%$ versus $31.3 \pm 1.2\%$ at 96 hours and $28.3 \pm 1.7\%$ versus $19.5 \pm 1.5\%$ at 168 hours; $P < 0.05$). By contrast, the frequency of TUNEL-positive cells was significantly reduced by cilostazol in each of the five LETO rats tested ($29.5 \pm 1.1\%$ versus $19.5 \pm 1.0\%$ at 24 hours after 2VO, $31.3 \pm 1.3\%$ versus $21.4 \pm 1.2\%$ at 48 hours, $19.4 \pm 1.1\%$ versus $10.3 \pm 1.5\%$ at 96 hours,

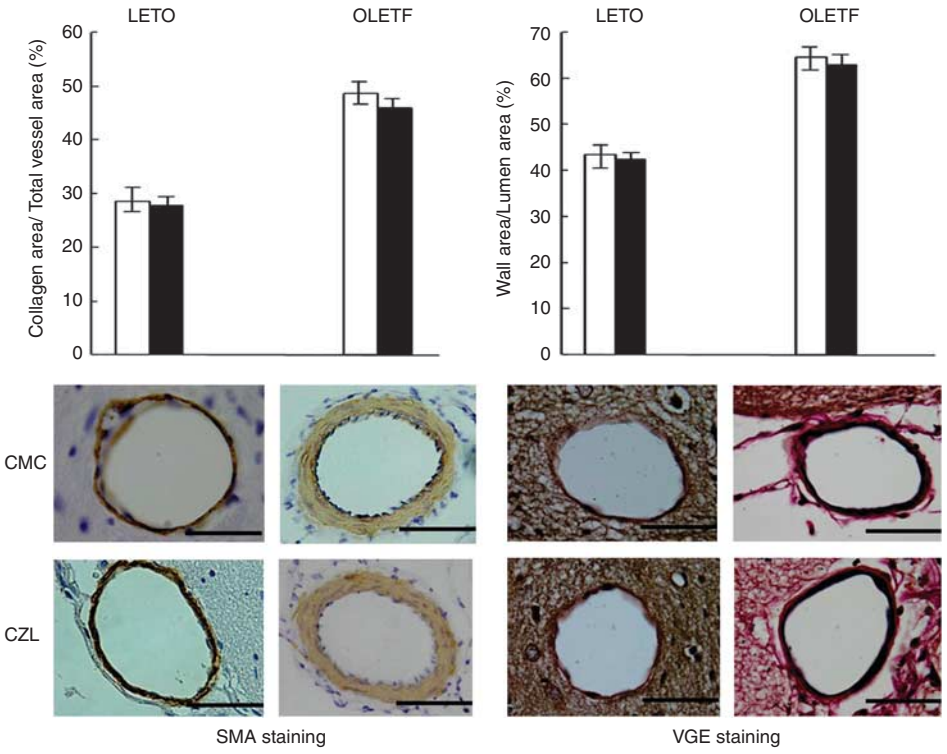

Figure 4 Comparison of the composition of cerebral small vessels between Otsuka Long-Evans Tokushima Fatty (OLETF) and Long-Evans Tokushima Otsuka (LETO) rats using smooth muscle actin (SMA) and Van Gieson's elastic (VGE) staining. Sections stained with VGE demonstrated a significantly higher ratio of collagen-stained tissue to total vessel area in OLETF versus LETO rats. This change in the small vessels of both LETO (28.6 ± 1.8% and 27.8 ± 1.5%) and OLETF (48.5 ± 1.7% and 45.9 ± 1.9%) rats was not affected by cilostazol (CZL) at 168 hours after 2VO. The ratio of wall thickness to luminal area was significantly higher in the OLETF rats than in the LETO rats. The wall thickness was not improved by CZL at 168 hours after 2VO in either LETO (43.3 ± 1.2% versus 42.4 ± 1.4%) or OLETF (64.5 ± 1.0% versus 63.0 ± 1.1%) rats (bar = 20 μm, × 1,000 magnification). The data for the CZL-administered groups are represented by dark bars and the data for the carboxymethyl cellulose (CMC)-administered groups are represented by light bars.

and 11.5 ± 1.9% versus 5.3 ± 1.6% at 168 hours; $P < 0.05$).

Figure 5 also illustrates the Bax expression near the infarct area in the cortical tissues. The overall percentage of cells that was immunopositive for Bax was higher in OLETF rats than in LETO rats, and was not reduced by cilostazol during the 48 hours after 2VO (52.4 ± 1.1% versus 49.2 ± 1.3% at 24 hours and 46.3 ± 1.0% versus 42.5 ± 1.3% at 48 hours), but was reduced significantly at 96 hours after 2VO (35.2 ± 1.2% versus 30.2 ± 1.0% at 96 hours and 28.4 ± 1.2% versus 18.9 ± 1.3% at 168 hours; $P < 0.05$). Similar to TUNEL staining, the percentage of Bax-positive cells was reduced by cilostazol in each of the five LETO rats tested (30.4 ± 1.2% versus 20.2 ± 1.3% at 24 hours after 2VO, 25.4 ± 1.1% versus 15.1 ± 1.0% at 48 hours, 20.1 ± 1.2% versus 9.5 ± 1.3% at 96 hours, and 10.5 ± 1.4% versus 5.1 ± 1.2% at 168 hours; $P < 0.05$).

By contrast, Figure 5 shows that there was little immunolabeling for Bcl-2 near the infarct area at 24 hours after 2VO in both LETO rats (5.0 ± 1.2% versus 7.4 ± 1.4%) and OLETF rats (4.1 ± 1.1% versus 6.4 ± 1.3%); however, the number of Bcl-2-positive cells gradually increased over time, and was significantly increased by cilostazol at 48 hours after 2VO in both LETO rats (6.4 ± 1.2% versus 10.2 ± 1.1% at 48 hours, 13.1 ± 1.4% versus 28.8 ± 1.5% at 96 hours, and 24.5 ± 1.3% versus 38.7 ± 1.5% at 168 hours; $P < 0.05$) and OLETF rats (5.6 ± 1.2% versus 9.4 ± 1.1% at 48 hours, 11.4 ± 1.3% versus 22.3 ± 1.4% at 96 hours, and 22.3 ± 1.5% versus 34.5 ± 1.3% at 168 hours; $P < 0.05$).

There were many AGE-positive cells in the OLETF rats (70.1 ± 5.4% versus 71.4 ± 4.8%) but comparatively few in the LETO rats (11.1 ± 6.4% versus 11.4 ± 5.1%) at 168 hours after 2VO with vehicle or cilostazol treatment (Figure 6).

Discussion

We examined the postadministration effects of cilostazol in a 2VO model. Cilostazol significantly reduced the infarct size and the number of apoptotic cells in the area surrounding the infarct 24, 48, 96, and 168 hours after 2VO in the LETO rats. However, the infarct size was not reduced by cilostazol 24 and 48 hours after 2VO in the OLETF rats. The infarct

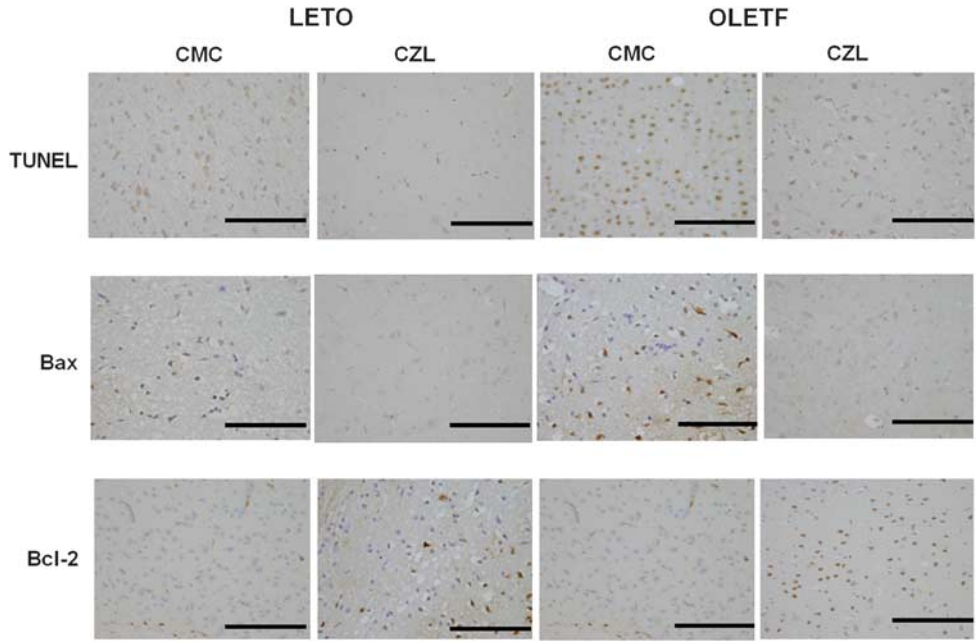

Figure 5 Terminal deoxynucleotidyl transferase-mediated deoxyuridine triphosphate nick-end labeling (TUNEL), Bax, B-cell lymphoma 2-associated X protein (Bax), and B-cell lymphoma 2 (Bcl-2) staining in the penumbra, and the effects of cilostazol (CZL) after 96 hours in Long-Evans Tokushima Otsuka (LETO) and Otsuka Long-Evans Tokushima Fatty (OLETF) rats. The number of apoptotic TUNEL-positive cells (with darkly stained nuclei or nuclear fragments with a cytoplasmic halo) was reduced by CZL. Strong Bax protein expression was observed both in the penumbra and in areas distant from the acute ischemic lesion, and was suppressed by CZL. Immunolabeling for Bcl-2 near the infarct area was increased by CZL (bar = 200 μm, $\times$200 magnification). CMC, carboxymethyl cellulose.

size was decreased by cilostazol 96 and 168 hours after 2VO, as was the number of apoptotic cells around the infarct core, in the OLETF rats. Multipoint measurement detected a beneficial effect of cilostazol on the ischemic CBF in the area of the cortex that might be perfused by collaterals (i.e., the ischemic penumbra). The improvement of the penumbral CBF might have contributed to the reduction of infarct size in the LETO rats. However, no CBF improvement was observed in the OLETF rats. The small-vessel morphology in the cortex was not changed by cilostazol in either of the rat strains: cilostazol did not affect the vessel wall thickness and narrow lumen areas revealed by SMA staining, the peri-vascular fibrosis and collagen deposition revealed by Van Gieson's elastic staining, and the increased AGE immunolabeling in the OLETF rats compared with the LETO rats. The extent of venous infarction and apoptosis was reduced at 24 hours after 2VO in the LETO rats due to the CBF improvement caused by cilostazol; however, the presence of lesions was also reduced after 96 hours in the OLETF rats, not as a result of CBF improvement but rather due to the activation of Bcl-2 by cilostazol.

In the OLETF rats, cilostazol induced a similar pattern of Bcl-2 expression to that seen in the LETO rats (in terms of both the timing and the level of expression); the expression of Bcl-2 might thus have

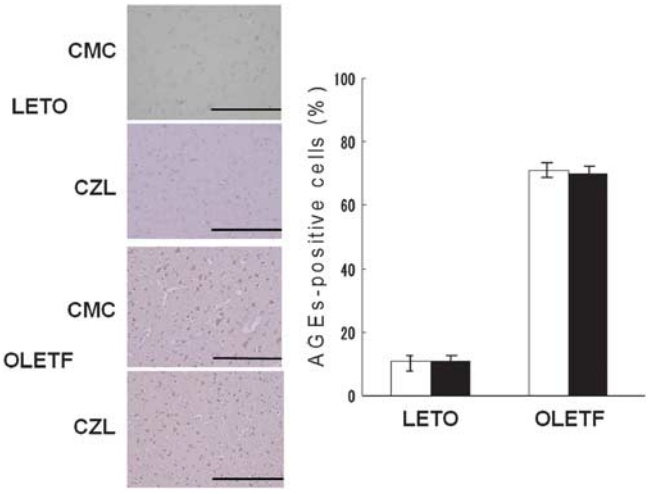

Figure 6 Advanced glycation end product (AGE) staining at 168 hours after the administration of cilostazol (CZL) in Long-Evans Tokushima Otsuka (LETO) and Otsuka Long-Evans Tokushima Fatty (OLETF) rats. AGEs were strongly expressed in OLETF rats, and were not suppressed by CZL (70.1 ± 5.4% versus 71.4 ± 4.8%). AGEs were more weakly expressed in LETO rats and were also not affected by CZL (11.1 ± 6.4% versus 11.4 ± 5.1%; bar = 200 μm, $\times$200 magnification). The data for the CZL-administered groups are represented by dark bars and the data for the carboxymethyl cellulose (CMC)-administered groups are represented by light bars.

a role in the protective effects of cilostazol against the brain damage induced by the 2VO model. The efficacy of cilostazol in the 2VO model could be largely attributable to mechanisms other than antiplatelet effects.

Venous Ischemia After Two-Vein Occlusion

A previous study confirmed that apoptosis due to venous ischemia appeared both in the center of the infarct and in remote areas (Nishioka *et al*, 2006). Congestion of the cerebral vein impairs the microcirculation in the cortical area, and the gradually expanding ischemic area further affects the CBF and unstable brain tissue. The area around the infarct lesion is at an incomplete ischemic stage, which might influence the function and condition of neurons. Venous ischemia, in particular, causes widespread changes and gradual alterations after venous occlusion, resulting in extensive apoptosis (Kempski *et al*, 1999). Venous ischemic neuronal death is characterized by cell swelling, and the inhibition of adenosine triphosphate synthesis occurs with the formation of nitric oxide radicals leading to necrosis in the infarct core. The circulation in the rat brain differs from that in the human such that the cortical collateral flow is sufficiently rich to maintain the CBF in the ischemic state induced by single vein occlusion (Nakase *et al*, 1996). However, venous ischemic neuronal death, as described above, in the normal and diabetic states can be evaluated in the 2VO model in rats.

A previous study using the 2VO model showed that the regional CBF between the two occluded veins had decreased significantly in diabetic OLETF rats compared with nondiabetic LETO rats by 90 minutes after occlusion (Wajima *et al*, 2010). We also previously showed that Bax expression in diabetic animals was further enhanced around the infarct area, consistent with an increase in apoptotic activity as indicated by a high degree of TUNEL-positive staining (Wajima *et al*, 2010). Our present study examined whether cilostazol attenuated the venous ischemic changes and widespread apoptotic changes around the infarct lesion, as shown in the MCAO model in rats, and whether these changes occurred in the diabetic state.

Efficacy of Cilostazol in Nondiabetic Rats

Our results revealed that cilostazol increased the regional CBF in nondiabetic LETO rats. Increased CBF in the ischemic region after the administration of cilostazol was reported previously in an MCAO model (Ito *et al*, 2009; Wainwright *et al*, 2007). Cilostazol is a selective inhibitor of phosphodiesterase-3. On inhibition of phosphodiesterase-3 activity and suppression of cyclic adenosine monophosphate) degradation, the intracellular cyclic adenosine monophosphate level increased in platelets and blood vessels, leading to the inhibition of platelet aggregation and the dilation of vascular smooth muscle cells. Through these vasodilating effects, the decrease of regional CBF induced by 2VO seemed to be rescued by cilostazol in nondiabetic rats.

Recently, cilostazol was shown to have pleiotropic effects other than antiplatelet and vasodilating activities (Ito *et al*, 2009). It inhibited the production of intracellular reactive oxygen species and apoptotic cell death in human umbilical vein endothelial cells. A reduction of oxidative stress by cilostazol might have contributed to the protection from brain injury after ischemia (Wainwright *et al*, 2007). In our current study, the infarct volume and numbers of TUNEL- and Bax-positive cells were decreased by cilostazol in the penumbra around the infarct lesion in the nondiabetic state. We considered the suppression of venous ischemic and brain apoptotic changes by cilostazol to be a dual effect of increasing the CBF via the dilatation of vessels, and the neuroprotective and antiinflammatory reactions described above. Previous reports showed that cilostazol treatment decreased the brain damage and cell apoptosis around the lesion after MCAO in rats (Ito *et al*, 2009; Nonaka *et al*, 2009).

Regarding the effects on vessels, cilostazol induced nitric oxide production from endothelial nitric oxide synthase (Wainwright *et al*, 2007). These endogenous vasodilating substances are protective in cerebral ischemic models. We did not confirm the vasodilating effect of endothelial nitric oxide synthase in 2VO and in the diabetic state; however, we believe that it was responsible for increasing the regional CBF to some extent in 2VO without changing the morphology of the cortical vessels in the nondiabetic LETO rats. In our study, the administration of cilostazol for 7 days did not change the morphology of small vessels in the cortical area. However, the regional CBF after 2VO was increased by cilostazol in the nondiabetic LETO rats. We attributed this CBF increase to the dilatation of vessels (i.e., main trunk vessels) other than the small vessels in the cortical regions.

Limited Efficacy of Cilostazol in Diabetic Rats

Previous studies showed that a combination of diabetes and MCAO resulted in more severe brain injury than MCAO alone due to enhanced apoptosis (Rizk *et al*, 2006). Previous reports (Lee *et al*, 2008) found that cilostazol exerts neuroprotective effects against transient focal ischemic brain injury. However, few reports have shown that cilostazol decreased the infarction after MCAO in diabetic rats.

In our current study, cilostazol did not improve the regional CBF improvement during the 4 hours after 2VO in diabetic OLETF rats. A previous study without the administration of cilostazol showed a greater degree of reduction of the CBF within ischemic areas in diabetic OLETF rats than in

nondiabetic LETO rats; this suggested that the diminished CBF also had a role in the more severe venous infarction and apoptosis seen in diabetic subjects (Wajima *et al*, 2010). Mechanisms that might explain the decreased regional CBF in the diabetic state were suggested in a previous study (Duckrow *et al*, 1987). The arterial oxygen content, which is determined in part by Ht, could be an important determinant of regional CBF. However, the Ht values, which are a major determinant of blood viscosity, did not significantly differ between the OLETF and LETO rats (and were not influenced by cilostazol). Previous studies have showed increased myogenic tone in experimental diabetes (Didion *et al*, 2005; Dumont *et al*, 2003). In addition to increased basal tone, the small cerebral vessels of diabetic rats exhibit reduced expression of the endothelium-derived relaxation factor, which might result in impaired vasodilatation. We predict that these factors might suppress the vasodilating effects of cilostazol in the diabetic state. Without an increase of CBF caused by cilostazol, its administration had no effect on the infarct volume and number of apoptotic cells in the early phase (during the 48 hours after administration) in the diabetic state.

Diabetes causes hypertrophic remodeling of the peripheral vasculature that is characterized by reduction of the lumen diameter, enlargement of the tunica media, abnormalities in the expression and localization of extracellular matrix components, such as collagen and laminin deposition in vessel walls and accelerated formation of atherosclerotic plaques, and intimal proliferation (Vinik and Flemmer, 2002). Our current results indicated a loss of cerebral capillaries and morphological changes of the smooth muscle within the cerebral cortex vasculature of OLETF rats. We observed thickening of small-vessel walls and perivascular fibrosis in the OLETF rats, which are typical cerebral microvascular atherosclerotic changes. Cilostazol did not affect these changes or any of the physiological data in our experiment. Hence, although a previous report suggested that cilostazol might improve atherosclerotic changes in medium-to-large vessels (Ling *et al*, 2006), it did not affect those seen in small vessels over 168 hours after administration. Alongside the diabetic suppression of vasodilating effects induced by cilostazol, this could explain why its administration did not increase the regional CBF after 2VO in diabetic OLETF rats.

AGE cytotoxicity was observed in the diabetic state. In the late stage of glycation, AGEs are formed after a complex cascade of repeated dehydration, condensation, fragmentation, oxidation, and cyclization reactions, via intermediates such as 3-deoxyglucosone (Kikuchi *et al*, 2003). Our results were consistent with previous reports showing increased AGE-positive immunolabeling in diabetic OLETF rats compared with nondiabetic LETO rats (Seki *et al*, 2003). In addition, due to AGE cytotoxicity, there were increased lesions and apoptotic changes in OLETF rats. The numbers of AGE-positive cells were not reduced by cilostazol. We therefore propose that cilostazol inhibited the inflammatory responses, but that the AGE cytotoxicity in neurons progressed slowly and was not affected. In summary, in the diabetic state, the extent of ischemic lesions and apoptotic changes increased after 2VO together with AGE cytotoxicity, and cilostazol reduced these changes.

Effects of B-Cell Lymphoma 2 Overexpression Induced by Cilostazol in Diabetic Rats

Our results suggested that diabetes exacerbated the neuronal death after cerebral ischemic injury caused by CBF reduction in areas with small-vessel atherosclerotic changes and the induction of apoptosis caused by AGE cytotoxicity; however, a reduction of infarct lesions induced by cilostazol via Bcl-2 was seen over time. In the presence of Bcl-2 overexpression, the infarct volume and the numbers of TUNEL- and Bax-positive cells were decreased by cilostazol in the late phase (i.e., after 96 hours).

Recently, cilostazol was shown to suppress the laddering feature of DNA fragmentation in a rat MCAO model (Ito *et al*, 2009). Accumulating evidence points to a significant role during apoptosis of Bcl-2 and cytochrome c release from mitochondria to the cytosol, and of caspase-3 activation in promoting cell survival and death (Chen *et al*, 2001). The overexpression of Bcl-2 in transgenic mice protected neurons from ischemia-induced cell death (Lee *et al*, 2008). Similarly, human Bcl-2 overexpression with herpes simplex virus vectors limited neuronal death in focal cerebral ischemia (Lee *et al*, 2008). Bcl-2 protects the integrity of mitochondrial dysfunction induced by cerebral apoptosis stimuli. A previous study showed that cilostazol treatment resulted in the overexpression of the phosphorylated cyclic adenosine monophosphate-responsive element binding protein and Bcl-2 after hypoperfusion (Lee *et al*, 2008). This finding suggests that the brain-protective role of cilostazol might be manifested through its antiapoptotic effect via the cyclic adenosine monophosphate-responsive element binding protein phosphorylation signaling pathway and the subsequent activation of Bcl-2.

Our current results were consistent with previous findings (Lee *et al*, 2008), in that cilostazol induced the activation of Bcl-2 after 2VO in both strains of rat. In the diabetic OLETF rats in particular, although the CBF after 2VO was not increased by cilostazol, the extent of venous infarction and apoptotic change was reduced after 168 hours. We attributed this to the activation of Bcl-2 by cilostazol.

Other potential mechanisms for the protective effect in the penumbral region induced by cilostazol were reported previously. Cilostazol was reported to suppress the breakdown of the blood–brain barrier after focal ischemia, to increase levels of

phosphorylated cyclic adenosine monophosphate-responsive element binding protein and cyclooxygenase-2, to suppress the activation of microglia and astrocytes, and to reduce the activation of oligodendrocytes, as well as decreasing tumor necrosis factor (TNF)-α and apoptosis in white-matter lesions in the bilateral common carotid artery ligation (BCCAL) rat model (Lee *et al*, 2008). These factors were not considered in the present experiment, although some might be related to the effect of cilostazol on the expression of Bcl-2.

In conclusion, we showed that cilostazol minimized venous ischemic injury in both diabetic and control rats. These findings suggest that cilostazol could be a potential therapeutic drug for use against diabetes-associated vascular disease, especially microvascular disease.

Acknowledgements

The authors thank the Tokushima Research Institute of Otsuka Pharmaceutical for supplying cilostazol, and OLETF and LETO rats.

Disclosure/conflict of interest

The authors declare no conflict of interest.

References

Chen Y, Ginis I, Hallenbeck JM (2001) The protective effect of ceramide in immature rat brain hypoxia-ischemia involves up-regulation of bcl-2 and reduction of TUNEL-positive cells. *J Cereb Blood Flow Metab* 21:34–40

Didion SP, Lynch CM, Baumbach GL, Faraci FM (2005) Impaired endothelium-dependent responses and enhanced influence of Rho-kinase in cerebral arterioles in type II diabetes. *Stroke* 36:342–7

Duckrow RB, Beard DC, Brennan RW (1987) Regional cerebral blood flow decreases during chronic and acute hyperglycemia. *Stroke* 18:52–8

Dumont AS, Dumont RJ, McNeill JH, Kassell NF, Sutherland GR, Verma S (2003) Chronic endothelin antagonism restores cerebrovascular function in diabetes. *Neurosurgery* 52:653–60; discussion 9–60

Ito H, Hashimoto A, Matsumoto Y, Yao H, Miyakoda G (2009) Cilostazol, a phosphodiesterase inhibitor, attenuates photothrombotic focal ischemic brain injury in hypertensive rats. *J Cereb Blood Flow Metab* 30:343–51

Kawano K, Hirashima T, Mori S, Saitoh Y, Kurosumi M, Natori T (1992) Spontaneous long-term hyperglycemic rat with diabetic complications. Otsuka Long-Evans Tokushima Fatty (OLETF) strain. *Diabetes* 41:1422–8

Kempski O, Seiwert T, Otsuka H, Heimann A, Nakase H (1999) Modelling of the ischemic penumbra. *Acta Neurochir Suppl* 73:41–4

Kikuchi S, Shinpo K, Takeuchi M, Yamagishi S, Makita Z, Sasaki N, Tashiro K (2003) Glycation: a sweet tempter for neuronal death. *Brain Res Brain Res Rev* 41:306–23

Kimura R, Nakase H, Tamaki R, Sakaki T (2005) Vascular endothelial growth factor antagonist reduces brain edema formation and venous infarction. *Stroke* 36:1259–63

Lee Y, Park S, Shin H, Kim C, Lee W, Hong K (2008) Protective effects of cilostazol against transient focal cerebral ischemia and chronic cerebral hypoperfusion injury. *CNS Neurosci Ther* 14:143–52

Ling G, Furong W, Bo W, Bendi G, Jie Z, Xiumei Z, Jiajun Z (2006) Cilostazol protects diabetic rats from vascular inflammation via nuclear factor-κB-dependent down-regulation of vascular cell adhesion molecule-1 expression. *J Pharmacol Exp Ther* 318:53–8

Nakagawa I, Alessandri B, Heimann A, Kempski O (2005) MitoKATP-channel opener protects against neuronal death in rat venous ischemia. *Neurosurgery* 57:334–40; discussion 334–40

Nakase H, Heimann A, Kempski O (1996) Local cerebral blood flow in a rat cortical vein occlusion model. *J Cereb Blood Flow Metab* 16:720–8

Nishioka T, Nakase H, Nakamura M, Konishi N, Sakaki T (2006) Sequential and spatial profiles of apoptosis in ischemic penumbra after two-vein occlusion in rats. *J Neurosurg* 104:938–44

Nonaka Y, Koumura A, Hyakkoku K, Shimazawa M, Yoshimura S, Iwama T, Hara H (2009) Combination treatment with normobaric hyperoxia and cilostazol protects mice against focal cerebral ischemia-induced neuronal damage better than each treatment alone. *J Pharmacol Exp Ther* 330:13–22

Otsuka H, Nakase H, Nagata K, Ueda K, Kempski O, Sakaki T (2000) Effect of age on cerebral venous circulation disturbances in the rat. *J Neurosurg* 93:298–304

Rizk NN, Rafols JA, Dunbar JC (2006) Cerebral ischemia-induced apoptosis and necrosis in normal and diabetic rats: effects of insulin and C-peptide. *Brain Res* 1096:204–12

Seki N, Hashimoto N, Sano H, Horiuchi S, Yagui K, Makino H, Saito Y (2003) Mechanisms involved in the stimulatory effect of advanced glycation end products on growth of rat aortic smooth muscle cells. *Metabolism* 52:1558–63

Shinohara Y, Katayama Y, Uchiyama S, Yamaguchi T, Handa S, Matsuoka K, Ohashi Y, Tanahashi N, Yamamoto H, Genka C, Kitagawa Y, Kusuoka H, Nishimaru K, Tsushima M, Koretsune Y, Sawada T, Hamada C (2010) For the CSPS 2 group Cilostazol for prevention of secondary stroke (CSPS 2): an aspirin-controlled, double-blind, randomised non-inferiority trial. *Lancet Neurol* 9:959–68

Vinik A, Flemmer M (2002) Diabetes and macrovascular disease. *J Diabetes Complications* 16:235–45

Wainwright MS, Grundhoefer D, Sharma S, Black SM (2007) A nitric oxide donor reduces brain injury and enhances recovery of cerebral blood flow after hypoxia-ischemia in the newborn rat. *Neurosci Lett* 415:124–9

Wajima D, Nakamura M, Horiuchi K, Miyake H, Takeshima Y, Tamura K, Motoyama Y, Konishi N, Nakase H (2010) Enhanced cerebral ischemic lesions after two-vein occlusion in diabetic rats. *Brain Res* 1309:126–35

Whisnant JP (1997) Modeling of risk factors for ischemic stroke. The Willis Lecture. *Stroke* 28:1840–4

SOME RIGHTS RESERVED This work is licensed under the Creative Commons Attribution-NonCommercial-Share Alike 3.0 Unported License. To view a copy of this license, visit http://creativecommons.org/licenses/by-nc-sa/3.0/